ISSN 1064-5624, Doklady Mathematics, 2023, Vol. 108, No. 1, pp. 300–308. © Pleiades Publishing, Ltd., 2023.
Russian Text © The Author(s), 2023, published in Doklady Rossiiskoi Akademii Nauk. Matematika, Informatika, Protsessy Upravleniya, 2023, Vol. 512, pp. 69–77.

MATHEMATICS

Hidden Boundary of Global Stability in a Counterexample to the Kapranov Conjecture on the Pull-In Range

Corresponding Member of the RAS N. V. Kuznetsov[a,b,*], M. Y. Lobachev[a,], and T. N. Mokaev[a]**

Received February 25, 2023; revised May 12, 2023; accepted May 22, 2023

Abstract—Within the framework of the development of the theory of hidden oscillations, the problem of determining the boundary of global stability and revealing its hidden parts corresponding to the nonlocal birth of hidden oscillations is considered. For a phase-locked loop with a proportional-integrating filter and a piecewise-linear phase detector characteristic, effective methods for determining bifurcations of global stability loss, for obtaining analytical formulas for bifurcation values, and for constructing trivial and hidden parts of the global stability boundary are suggested.

Keywords: hidden boundary of global stability, self-excited and hidden oscillations, local and global bifurcations, phase-locked loop, Kapranov conjecture, pull-in range

DOI: 10.1134/S1064562423700898

1. INTRODUCTION

A key engineering problem in nonlinear analysis of phase-locked loops (PLLs) is the determination of the pull-in range for the input signal frequency depending on physical implementation parameters of the system [1, 2]. For given physical implementation parameters and input signal frequency corresponding to the pull-in range, the state of the system with any initial data is attracted to a stationary set, and the system is called globally stable [3].[1] The boundary of global stability in the parameter space of the system is the boundary of the closure of the set of parameters for which the system is not globally stable (in the phase space, there are trajectories that do not tend to the stationary set). Moreover, points of the boundary of global stability are bifurcation points[2] corresponding to the birth of undamped oscillations that do not tend to the stationary set. A point of the global stability boundary is called *hidden* [4] if for its certain neighborhood in the parameter space the loss of global stability is caused only by global bifurcations of the birth of *hidden oscillations* for which the basin of attraction in the phase space is not connected with unstable equilibria; otherwise, the point is called *trivial* (*explicit*). Trivial points of the global stability boundary can be determined using well-developed methods for analyzing local bifurcations and numerical procedures for analyzing self-excited oscillations in a neighborhood of unstable points of the stationary set. General methods for determination of hidden points of the global stability boundary require nonlocal analysis, including analysis of global bifurcations, and such methods are developed in the theory of hidden oscillations [4, 5].

For a PLL system with a proportional-integrating filter, in Kapranov's 1956 paper [6], it was assumed (by analogy with the Tricomi problem [7]) that self-excited oscillations arising in the birth of a heteroclinic orbit connecting unstable saddle equilibria determine the loss of global stability and specify the pull-in range of the system (*Kapranov's conjecture*). However, it was soon shown that Kapranov's conjecture does not hold in the general case (see [8–11]) and the system can exhibit bifurcations of nonlocal birth of oscillations leading to the loss of global stability. Based on these results, series of bifurcation diagrams for some parameter values and phase detector characteristic types were numerically constructed in the 1970 paper [12]; however, it was noted that, in the general case, there are no sufficiently complete and detailed formulas for

[1] For systems with a nonunique equilibrium state, various types of stability can be defined depending on the character of attraction and the form of the stationary set; in this case, the terms *global asymptotic stability of a system* and a *gradient-type system* are also used for PLLs in [2, 18].

[2] For a *bifurcation point* in the parameter space of the system in an arbitrarily small neighborhood, there is another point such that the corresponding phase portraits of the system are not topologically equivalent. The nonequivalence of the phase portraits in an arbitrarily small neighborhood of a stationary set corresponds to a *local bifurcation*, and, outside such a neighborhood, to a *global bifurcation*.

[a] *St. Petersburg State University, St. Petersburg, Russia*
[b] *Institute for Problems in Mechanical Engineering, Russian Academy of Sciences, St. Petersburg, Russia*
**e-mail: n.v.kuznetsov@spbu.ru*
***e-mail: mlobachev64@gmail.com*

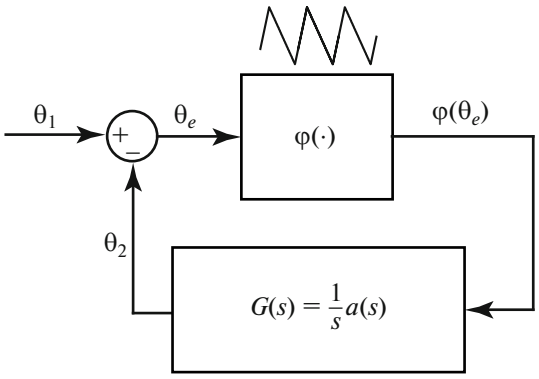

Fig. 1. PLL model in the form of a nonlinear control system.

fast computation of the pull-in range in the literature. As a result, at present, classical monographs on phase synchronization for the pull-in range of PLLs with a proportional-integrating filter offer copied numerical bifurcation diagrams, approximate or conservative analytical estimates, and remarks on the lack of a satisfactory solution to the problem (see, e.g., [1, 2, 13, 14]).

Below, to solve this problem within the framework of the theory of hidden oscillations, we develop an effective approach [15, 16] for determining the exact boundary of global stability and its hidden parts. The approach is based on a special change of variables, followed by integration and matching of trajectories in terms of phase variables. In contrast to [6, 8, 10, 11], this approach does not require the computation of time intervals for which trajectories pass through linearity intervals of the system, which simplifies the analysis and makes it visual. Developing these ideas in the present paper, we analytically describe all possible bifurcations of the loss of global stability, including global bifurcations of the birth of hidden oscillations, and derive complete analytical formulas for constructing trivial and hidden parts of the global stability boundary and for determining the pull-in range in the general case of a continuous piecewise-linear phase detector characteristic.

2. MATHEMATICAL MODEL AND FORMULATION OF THE PROBLEM

A classical PLL model in the signal's phase space can be written as a control system in the Lurie form [4]:

$$\dot{u} = Pu - q\varphi(r^{\mathrm{T}}u), \quad u = (u_1, u_2)^{\mathrm{T}} \in \mathbb{R}^2,$$
$$P = \begin{pmatrix} \dfrac{-1}{\tau_1+\tau_2} & 0 \\ \dfrac{-K_{\mathrm{vco}}}{\tau_1+\tau_2} & 0 \end{pmatrix}, \quad q = \begin{pmatrix} -\dfrac{\tau_1}{\tau_1+\tau_2} \\ \dfrac{K_{\mathrm{vco}}\tau_2}{\tau_1+\tau_2} \end{pmatrix}, \qquad (1)$$
$$r^{\mathrm{T}} = (0, 1), \quad \varphi(\cdot) = v_e(\cdot) - \frac{\omega_e^{\mathrm{free}}}{K_{\mathrm{vco}}},$$

where $K_{\mathrm{vco}} > 0$ is the gain of the voltage-controlled oscillator (VCO); ω_e^{free} is the difference between the input signal frequency and the natural frequency of the VCO; $\tau_1 > 0$, $\tau_2 \geq 0$ are parameters of a low-pass filter with the transfer function

$$F(s) = \frac{1+\tau_2 s}{1+(\tau_1+\tau_2)s};$$

the state of system (1) corresponds to a shifted state of the low-pass filter and to the phase difference between the input and voltage controlled signals: $u(t) = \left(x(t) - \dfrac{\tau_1\omega_e^{\mathrm{free}}}{K_{\mathrm{vco}}}, \theta_e(t)\right)^{\mathrm{T}}$; and $v_e(\cdot)$ is the phase detector characteristic, which is assumed in this paper to be continuous and piecewise-linear:

$$v_e(u_2) = \begin{cases} ku_2 - 2\pi km \\ -\dfrac{1}{k} + 2\pi m \leq u_2 < \dfrac{1}{k} + 2\pi m \\ -\dfrac{1}{\pi - \frac{1}{k}}u_2 + \dfrac{1}{\pi - \frac{1}{k}}(\pi + 2\pi m) \\ \dfrac{1}{k} + 2\pi m \leq u_2 < -\dfrac{1}{k} + 2\pi(m+1), \end{cases} \qquad (2)$$
$$k > \frac{1}{\pi}, \quad m \in \mathbb{Z}.$$

The triangular characteristic (2) with $k = \dfrac{2}{\pi}$ is obtained by analyzing impulse signals in digital electronics [2].

System (1) is associated with the block diagram shown in Fig. 1, where

$$\theta_1(t) - \theta_2(t) = \theta_e(t),$$
$$G(s) = r^T(sI - P)^{-1}q = \frac{1}{s}K_{\mathrm{vco}}F(s).$$

Due to the invariance of system (1) under the transformation $(\omega_e^{\mathrm{free}}, x(t), \theta_e(t)) \to (-\omega_e^{\mathrm{free}}, -x(t), -\theta_e(t))$, the analysis can be performed only for $\omega_e^{\mathrm{free}} \geq 0$. The equilibrium states of system (1) are described by the equations

$$u_1^{\mathrm{eq}} = 0, \quad v_e(u_2^{\mathrm{eq}}) = \frac{\omega_e^{\mathrm{free}}}{K_{\mathrm{vco}}}. \qquad (3)$$

The form of the function $v_e(\cdot)$ implies that, for $\omega_e^{\mathrm{free}} > K_{\mathrm{vco}}$, system (1) has no equilibria, and an analysis of the corresponding characteristic polynomials for

$\omega_e^{\text{free}} < K_{\text{vco}}$ implies that the equilibria $\left(0, \frac{\omega_e^{\text{free}}}{kK_{\text{vco}}} + 2\pi m\right)$ are asymptotically stable, while the equilibria $\left(0, \pi - (\pi k - 1)\frac{\omega_e^{\text{free}}}{kK_{\text{vco}}} + 2\pi m\right)$ are unstable for any $m \in \mathbb{Z}$.

The existence of an asymptotically stable equilibrium varying continuously in the phase space as ω_e^{free} varies continuously within the longest symmetric interval, $|\omega_e^{\text{free}}| \in [0, \omega_h)$, corresponds to the engineering concept of a *hold-in range* [17]. For system (1), we have $[0, \omega_h) = [0, K_{\text{vco}})$.

One of the key engineering problems in nonlinear analysis of PLLs is the estimation of the *pull-in range* $[0, \omega_p)$ [17], which is a subinterval of the hold-in range such that, for any initial data, the state of the system tends to an equilibrium. Note that the mathematical model admits unstable transient processes from a measure zero set of points of the phase space to unstable equilibria that are not observable in a physical implementation because of the noise.

3. MAIN RESULT

Applying qualitative methods for analysis of dynamical systems to the continuous piecewise-linear system (1), we can show that the loss of global stability is determined by bifurcations of disappearance of equilibria and the birth of a semistable cycle of the second kind[3] or a heteroclinic orbit connecting unstable saddle equilibria, but the loss of global stability is not connected with the birth of a cycle of the first kind or a homoclinic orbit [2, 18].

Let us define

$$\begin{aligned} K_{\text{vco}}^{\text{ht}} &= \frac{1}{k(2\tau_1 + \tau_2 + 2\sqrt{\tau_1(\tau_1 + \tau_2)})}, \quad \tau_2 \geq 0, \\ K_{\text{vco}}^{\text{fn}} &= \frac{1}{k(2\tau_1 + \tau_2 - 2\sqrt{\tau_1(\tau_1 + \tau_2)})}, \quad \tau_2 > 0, \end{aligned} \tag{4}$$

which determine the type of stable equilibria in terms of the parameter K_{vco}.

[3] A cycle of the first kind is a periodic trajectory in $\mathbb{R}^2$, and for cycles of the second kind $(u_1(t), u_2(t))$ there exists a period $T > 0$ and a number $\varepsilon = \pm 1$ such that $u_1(t + T) = u_1(t)$, $u_2(t + T) = u_2(t) + 2\pi\varepsilon$ $\forall t > 0$ [18].

Theorem 1. *For* $\tau_1 > 0$, $\tau_2 \geq 0$, $k > \frac{1}{\pi}$, *and* $K_{\text{vco}} \in (0, K_{\text{vco}}^{\text{ht}}]$, *the pull-in range coincides with the hold-in range*:

$$[0, \omega_p) = [0, \omega_h) = [0, K_{\text{vco}}).$$

Proof sketch. By making the changes of variables

$$y = \frac{\tau_2}{\sqrt{(\tau_1 + \tau_2)K_{\text{vco}}}}\omega_e^{\text{free}} - \sqrt{\frac{K_{\text{vco}}}{\tau_1 + \tau_2}}(u_1 + \tau_2 v_e(u_2)),$$
$$t \mapsto \sqrt{\frac{\tau_1 + \tau_2}{K_{\text{vco}}}}t,$$

system (1) on smoothness intervals can be written as

$$\begin{aligned} \dot{y} &= -\frac{1 + \tau_2 K_{\text{vco}} v_e'(\theta_e)}{\sqrt{(\tau_1 + \tau_2)K_{\text{vco}}}}y + \frac{\omega_e^{\text{free}}}{K_{\text{vco}}} - v_e(\theta_e), \\ \dot{\theta}_e &= y. \end{aligned} \tag{5}$$

Using a quadratic Lyapunov function for system (1) and analyzing the phase space, we find the absorbing set

$$\begin{aligned} \Omega = \Bigg\{ &(y, \theta_e) \in \mathbb{R}^2 \,|\, 0 \leq y \\ &\leq \sqrt{(\tau_1 + \tau_2)K_{\text{vco}}}\left(1 + \frac{\omega_e^{\text{free}}}{K_{\text{vco}}}\right)\Bigg\}, \end{aligned} \tag{6}$$

which contains the limit trajectories of system (5).

For $K_{\text{vco}} \in (0, K_{\text{vco}}^{\text{ht}}]$, the stable equilibria are nodes and their eigenvectors are the phase trajectories of (5) on linearity intervals. Since the trajectory corresponding to one of the eigenvectors of a node crosses domain (6) from boundary to boundary, there are no cycles of the second kind in system (5) and the pull-in range coincides with the hold-in range.

By applying the method of comparison systems (see, e.g., [18, 19]), a similar result on the coincidence of the pull-in and hold-in ranges in some domain of parameters can also be proved for a sinusoidal phase detector characteristic.

Lemmas 1 and 2 below describe bifurcations of the birth of a saddle-to-saddle heteroclinic orbit and a semistable limit cycle of the second kind for various values of $K_{\text{vco}} > K_{\text{vco}}^{\text{ht}}$.

Lemma 1. *Given* $\tau_1 > 0$, $\tau_2 \geq 0$, *and* $k > \frac{1}{\pi}$, *for any* $K_{\text{vco}} > K_{\text{vco}}^{\text{ht}}$, *there exists a unique value* $\omega_e^{\text{free}} = \omega^{\text{ht}} \in [0, K_{\text{vco}})$ *for which system* (1) *has a heteroclinic orbit connecting saddle equilibria, where*

$$\omega^{\mathrm{ht}} = \frac{\sqrt{s_1}-1}{\sqrt{s_1}+1}K_{\mathrm{vco}},$$

$$s_1 = \begin{cases} \dfrac{(\kappa-\eta)^2+2\xi(\kappa-\eta)+k}{(\kappa+\eta)^2-2\xi(\kappa+\eta)+k}\exp\left(\dfrac{2\xi}{\rho}\left(\arctan\dfrac{(\xi-\eta)^2+\rho^2-\kappa^2}{2\rho\kappa}+\dfrac{\pi}{2}\right)\right) \\ \text{if} \quad K_{\mathrm{vco}} \in (K_{\mathrm{vco}}^{\mathrm{ht}}, K_{\mathrm{vco}}^{\mathrm{fn}}) \quad \text{or} \quad \tau_2 = 0, \\ \left(\dfrac{\kappa-\eta+\sqrt{k}}{\kappa+\eta-\sqrt{k}}\exp\left(\dfrac{2\sqrt{k}\kappa}{\kappa^2-(\eta-\sqrt{k})^2}\right)\right)^2 \quad \text{if} \quad K_{\mathrm{vco}} = K_{\mathrm{vco}}^{\mathrm{fn}} \quad \text{and} \quad \tau_2 \neq 0, \\ \dfrac{(\kappa-\eta+\xi)^2-\rho^2}{(\kappa+\eta-\xi)^2-\rho^2}\left(\dfrac{(\kappa+\rho)^2-(\xi-\eta)^2}{(\kappa-\rho)^2-(\xi-\eta)^2}\right)^{\frac{\xi}{\rho}} \quad \text{if} \quad K_{\mathrm{vco}} > K_{\mathrm{vco}}^{\mathrm{fn}} \quad \text{and} \quad \tau_2 \neq 0, \end{cases} \tag{7}$$

$$\xi = \frac{k\tau_2 K_{\mathrm{vco}}+1}{2\sqrt{(\tau_1+\tau_2)K_{\mathrm{vco}}}}, \quad \eta = \frac{k\tau_2 K_{\mathrm{vco}}-\mu}{2\sqrt{(\tau_1+\tau_2)K_{\mathrm{vco}}}},$$
$$\rho = \sqrt{|\xi^2-k|}, \quad \kappa = \sqrt{\eta^2+k\mu}, \quad \mu = \pi k-1. \tag{8}$$

For $\tau_2 > 0$, we define

$$K_{\mathrm{vco}}^{\mathrm{pt}} = \frac{\pi k-1}{k\tau_2}. \tag{9}$$

Lemma 2. *Given* $\tau_1 > 0$, $\tau_2 > 0$, *and* $k > \frac{1}{\pi}$, *for any* $K_{\mathrm{vco}} > \max(K_{\mathrm{vco}}^{\mathrm{pt}}, K_{\mathrm{vco}}^{\mathrm{ht}})$, *there exists a unique value* $\omega_e^{\mathrm{free}} = \omega^{\mathrm{pt}} \in [0, K_{\mathrm{vco}})$ *for which system* (1) *has a semistable cycle of the second kind, where*

$$\omega^{\mathrm{pt}} = \frac{\sqrt{s_2}-1}{\sqrt{s_2}+1}K_{\mathrm{vco}},$$

$$s_2 = \frac{(z_0^{\mathrm{pt}}+\eta)^2-\kappa^2}{(z_1^{\mathrm{pt}}-\eta)^2-\kappa^2}\left(\frac{(z_0^{\mathrm{pt}}+\kappa+\eta)(z_1^{\mathrm{pt}}+\kappa-\eta)}{(z_0^{\mathrm{pt}}+\eta-\kappa)(z_1^{\mathrm{pt}}-\eta-\kappa)}\right)^{\frac{\eta}{\kappa}}, \tag{10}$$

$$z_0^{\mathrm{pt}} = z_0(z_1^{\mathrm{pt}}),$$
$$z_0(z_1) = \frac{(1+\mu)kz_1-2(\mu\xi+\eta)k}{(1+\mu)k-2(\xi-\eta)z_1},$$

and $z_1^{\mathrm{pt}} \in (\eta+\kappa, k\sqrt{\tau_2 K_{\mathrm{vco}}}]$ *is determined by the following transcendental equation for* z_1:

$$\frac{(z_0(z_1)+\eta)^2-\kappa^2}{(z_1-\eta)^2-\kappa^2}\left(\frac{(z_0(z_1)+\eta+\kappa)(z_1+\kappa-\eta)}{(z_0(z_1)+\eta-\kappa)(z_1-\eta-\kappa)}\right)^{\frac{\eta}{\kappa}}$$
$$= \begin{cases} \dfrac{(z_0(z_1))^2+2\xi z_0(z_1)+k}{z_1^2-2\xi z_1+k}\exp\left(\dfrac{2\xi}{\rho}\left(\arctan\dfrac{\rho}{z_0(z_1)+\xi}-\arctan\dfrac{z_1-\xi}{\rho}+\dfrac{\pi}{2}\right)\right) \\ \text{if} \quad K_{\mathrm{vco}} \in (K_{\mathrm{vco}}^{\mathrm{ht}}, K_{\mathrm{vco}}^{\mathrm{fn}}), \\ \left(\dfrac{z_0(z_1)+\sqrt{k}}{z_1-\sqrt{k}}\exp\left(\dfrac{\sqrt{k}}{z_0(z_1)+\sqrt{k}}+\dfrac{\sqrt{k}}{z_1-\sqrt{k}}\right)\right)^2 \quad \text{if} \quad K_{\mathrm{vco}} = K_{\mathrm{vco}}^{\mathrm{fn}}, \\ \dfrac{(z_0(z_1)+\xi)^2-\rho^2}{(z_1-\xi)^2-\rho^2}\left(\dfrac{(z_0(z_1)+\rho+\xi)(z_1+\rho-\xi)}{(z_0(z_1)+\xi-\rho)(z_1-\xi-\rho)}\right)^{\frac{\xi}{\rho}} \quad \text{if} \quad K_{\mathrm{vco}} > K_{\mathrm{vco}}^{\mathrm{fn}}. \end{cases}$$

Here, ξ, η, ρ, κ, $K_{\mathrm{vco}}^{\mathrm{fn}}$, $K_{\mathrm{vco}}^{\mathrm{ht}}$, $K_{\mathrm{vco}}^{\mathrm{pt}}$ *are defined formulas* (4), (8), *and* (9).

Lemma 2 can also be used to determine initial data for a semistable cycle if $\omega_e^{\mathrm{free}} = \omega^{\mathrm{pt}}$: $u(0) = \left(\left(k\tau_2 - \sqrt{\dfrac{\tau_1+\tau_2}{K_{\mathrm{vco}}}}\right)\left(\dfrac{1}{k}+\dfrac{\omega^{\mathrm{pt}}}{kK_{\mathrm{vco}}}\right)z_1^{\mathrm{pt}}, -\dfrac{1}{k}\right)$.

Theorem 2. *For* $\tau_1 > 0$, $k > \frac{1}{\pi}$, *and* $K_{\mathrm{vco}} > 0$, *the pull-in range of system* (1) *with piecewise-linear characteristic* (2) *has the following form*: *for* $\tau_2 = 0$,

$$[0, \omega_p) = \begin{cases} [0, K_{\mathrm{vco}}) & \text{if} \quad K_{\mathrm{vco}} \leq K_{\mathrm{vco}}^{\mathrm{ht}} \\ [0, \omega^{\mathrm{ht}}) & \text{if} \quad K_{\mathrm{vco}} > K_{\mathrm{vco}}^{\mathrm{ht}} \end{cases}$$

and, for $\tau_2 > 0$,

$$[0, \omega_p) = \begin{cases} [0, K_{\mathrm{vco}}) & \text{if} \quad K_{\mathrm{vco}} \le K_{\mathrm{vco}}^{\mathrm{ht}} \\ [0, \omega^{\mathrm{ht}}) & \text{if} \quad K_{\mathrm{vco}} \in (K_{\mathrm{vco}}^{\mathrm{ht}}, \max(K_{\mathrm{vco}}^{\mathrm{pt}}, K_{\mathrm{vco}}^{\mathrm{ht}})] \\ [0, \omega^{\mathrm{pt}}) & \text{if} \quad K_{\mathrm{vco}} > \max(K_{\mathrm{vco}}^{\mathrm{pt}}, K_{\mathrm{vco}}^{\mathrm{ht}}), \end{cases}$$

where ω^{ht} *and* ω^{pt} *are given by formulas* (7) *and* (10) (*here*, $\omega^{\mathrm{pt}} < \omega^{\mathrm{ht}}$ *for* $K_{\mathrm{vco}} > \max(K_{\mathrm{vco}}^{\mathrm{pt}}, K_{\mathrm{vco}}^{\mathrm{ht}})$).

Proof sketch. The case $K_{\mathrm{vco}} \le K_{\mathrm{vco}}^{\mathrm{ht}}$ was treated in Theorem 1. For $K_{\mathrm{vco}} > K_{\mathrm{vco}}^{\mathrm{ht}}$, we consider system (5) on a period and divide the phase portrait into the domains

- $A = \left\{(y, \theta_e) | \frac{1}{k} - 2\pi \le \theta_e < -\frac{1}{k}, y \in \mathbb{R}\right\}$,
- $B = \left\{(y, \theta_e) | -\frac{1}{k} \le \theta_e \le \frac{1}{k}, y \in \mathbb{R}\right\}$,

where system (5) is linear (see Fig. 2). Consider the trajectory $(y(t), \theta_e(t))$ intersecting the lines $\theta_e = \frac{1}{k} - 2\pi$, $\theta_e = -\frac{1}{k}$, and $\theta_e = \frac{1}{k}$ at the points $(y, \theta_e) = \left(y_0, \frac{1}{k} - 2\pi\right)$, $(y, \theta_e) = \left(y_1, -\frac{1}{k}\right)$, and $(y, \theta_e) = \left(y_2, \frac{1}{k}\right)$, respectively (see Fig. 2). By making the change of variables

$$z = \frac{\mu y}{\theta_e + \pi + \mu \dfrac{\omega_e^{\mathrm{free}}}{kK_{\mathrm{vco}}}},$$

$$\theta_e \in \left[\frac{1}{k} - 2\pi, -\pi - \mu\frac{\omega_e^{\mathrm{free}}}{kK_{\mathrm{vco}}}\right) \cup \left(-\pi - \mu\frac{\omega_e^{\mathrm{free}}}{kK_{\mathrm{vco}}}, -\frac{1}{k}\right),$$

$$z = \frac{y}{\theta_e - \dfrac{\omega_e^{\mathrm{free}}}{kK_{\mathrm{vco}}}}, \quad \theta_e \in \left[-\frac{1}{k}, \frac{\omega_e^{\mathrm{free}}}{kK_{\mathrm{vco}}}\right) \cup \left(\frac{\omega_e^{\mathrm{free}}}{kK_{\mathrm{vco}}}, \frac{1}{k}\right),$$

where $\mu = \pi k - 1$ (see (8)), system (5) can be written as equations with separated variables:

$$\frac{zdz}{z^2 - 2\eta z - \mu k} = -\frac{d\theta_e}{\theta_e + \pi + \mu \dfrac{\omega_e^{\mathrm{free}}}{kK_{\mathrm{vco}}}},$$

$$\theta_e \in \left[\frac{1}{k} - 2\pi, -\pi - \mu\frac{\omega_e^{\mathrm{free}}}{kK_{\mathrm{vco}}}\right) \cup \left(-\pi - \mu\frac{\omega_e^{\mathrm{free}}}{kK_{\mathrm{vco}}}, -\frac{1}{k}\right),$$

$$\frac{zdz}{z^2 + 2\xi z + k} = -\frac{d\theta_e}{\theta_e - \dfrac{\omega_e^{\mathrm{free}}}{kK_{\mathrm{vco}}}}, \tag{11}$$

$$\theta_e \in \left[-\frac{1}{k}, \frac{\omega_e^{\mathrm{free}}}{kK_{\mathrm{vco}}}\right) \cup \left(\frac{\omega_e^{\mathrm{free}}}{kK_{\mathrm{vco}}}, \frac{1}{k}\right),$$

and we can obtain expressions[4] describing the parts of the trajectory $(y(t), \theta_e(t))$ of system (5) in the domains A and B.

For y_1 corresponding to trajectories lying above the saddle's eigenvectors, the resulting expressions can be used to analytically determine the curves $y_0 = y_0(y_1)$ and $y_2 = y_2(y_1)$, the intersection of which corresponds to a cycle of the second kind with initial data $(y(0), \theta_e(0)) = \left(y_1, -\frac{1}{k}\right)$. Analyzing the derivatives of the curves $y_0(y_1)$, $y_2(y_1)$ and restricting the search domain by set (6) and the additional condition that the trajectories pass above the saddle's eigenvectors, we can derive analytical formulas for the bifurcation value $\omega_e^{\mathrm{free}} = \omega^{\mathrm{pt}}$ determining the boundary of global stability of system (1) for $K_{\mathrm{vco}} > \max(K_{\mathrm{vco}}^{\mathrm{pt}}, K_{\mathrm{vco}}^{\mathrm{ht}})$.

Similarly, we consider the limiting case when a heteroclinic orbit connecting saddle equilibria arises in the system. An analysis of the saddle's eigenvectors yields the points $y_1^{\mathrm{ht}} = (\kappa + \eta)\left(\frac{1}{k} + \frac{\omega_e^{\mathrm{free}}}{kK_{\mathrm{vco}}}\right)$ and $y_2^{\mathrm{ht}} = (\kappa - \eta)\left(\frac{1}{k} - \frac{\omega_e^{\mathrm{free}}}{kK_{\mathrm{vco}}}\right)$, at which the heteroclinic orbit intersects the lines $\theta_e = -\frac{1}{k}$ and $\theta_e = \frac{1}{k}$, respectively. Substituting the points $\left(y_1^{\mathrm{ht}}, -\frac{1}{k}\right)$ and $\left(y_2^{\mathrm{ht}}, \frac{1}{k}\right)$ into the analytical expression for trajectories in the domain B, we determine the bifurcation value $\omega_e^{\mathrm{free}} = \omega^{\mathrm{ht}}$.

Thus, for $K_{\mathrm{vco}} > K_{\mathrm{vco}}^{\mathrm{ht}}$, the pull-in range is determined by the fact that the point $(y_1^{\mathrm{ht}}, y_0^{\mathrm{ht}})$ of $y_0(y_1)$ belongs to the curve $y_2 = y_2(y_1)$ (see Fig. 2) at $\omega_e^{\mathrm{free}} = \omega^{\mathrm{ht}}$ (7), which corresponds to the birth of a saddle-to-saddle heteroclinic orbit, or by the fact that the curves are tangent at $\omega_e^{\mathrm{free}} = \omega^{\mathrm{pt}}$ (10), which corresponds to the birth of a semistable cycle.

Corollary 1. *Fix* $a = \frac{\tau_2}{\tau_1 + \tau_2} \in (0, 1)$. *Then*

$$\frac{\omega_p}{K_{\mathrm{vco}}} \to \frac{-2ab + b^2 + a}{2b - b^2 - a} \quad \text{as} \quad (\tau_1 + \tau_2)K_{\mathrm{vco}} \to +\infty, \tag{12}$$

[4] For a trajectory of system (5) intersecting the discontinuity line $\theta_e = -\pi - \mu\frac{\omega_e^{\mathrm{free}}}{kK_{\mathrm{vco}}}$ or $\theta_e = \frac{\omega_e^{\mathrm{free}}}{kK_{\mathrm{vco}}}$, based on the continuity of the trajectories of the system, with a suitable choice of the constant of integration, the parts of the solution specified by Eqs. (11) are matched.

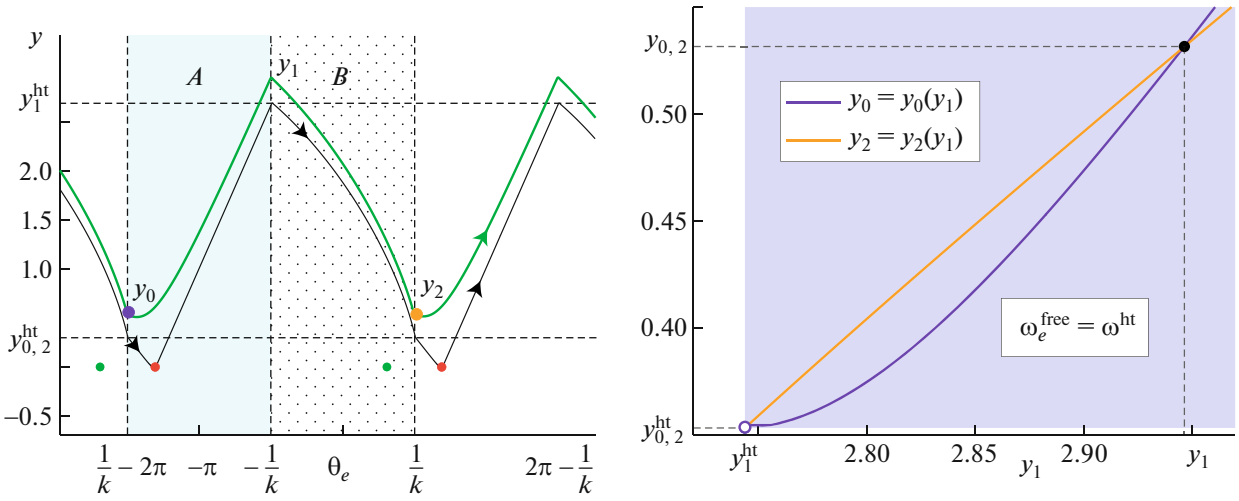

Fig. 2. The point $(y_1^{ht}, y_0^{ht}) = (2.744, 0.353)$ of the curve $y_0 = y_0(y_1)$ gets to the curve $y_2 = y_2(y_1)$, which corresponds to a heteroclinic orbit with initial data $(y(0), \theta_e(0)) = \left(2.744, -\frac{1}{k}\right)$ that connects saddle equilibria in system (5). The intersection of the curves $y_0 = y_0(y_1)$ and $y_2 = y_2(y_1)$ at the point $(y_1, y_0) = (2.946, 0.531)$ corresponds to a stable cycle of the second kind in system (5) with initial data $(y(0), \theta_e(0)) = \left(2.946, -\frac{1}{k}\right)$. Parameters: $k = \frac{2}{\pi}$, $\tau_1 = 0.0448$, $\tau_2 = 0.0185$, $K_{vco} = 250$, and $\omega_e^{free} = \omega^{ht} \approx 154.77$.

where $b \in (a, \sqrt{a}]$ is a unique solution of the equation

$$\frac{a(2b - a - b^2)}{b(b-a)} = \ln \frac{b^2(1-a)}{(b-a)^2}.$$

If $\tau_2 = 0$, then $\frac{\omega_p}{K_{vco}} \to 0$ as $\tau_1 K_{vco} \to +\infty$.

4. COUNTEREXAMPLE TO KAPRANOV'S CONJECTURE: HIDDEN AND TRIVIAL PARTS OF THE GLOBAL STABILITY BOUNDARY

For fixed $k > \frac{1}{\pi}$, after making a change of variables and introducing the parameter $a = \frac{\tau_2}{\tau_1 + \tau_2}$, bifurcation diagrams with axes $\left((\tau_1 + \tau_2)K_{vco}, \frac{\omega_e^{free}}{K_{vco}}\right)$ for various values of a can be constructed using Theorem 2 (for the code plotting bifurcation diagrams, see https://github.com/ApCyb/2023-PLL-lead-lag-pull-in).

Figure 3 shows the boundary of global stability constructed using the analytical expressions from Theorem 2 for the standard engineering parameter values $\tau_1 = 0.0448$, $\tau_2 = 0.0185$ [20] and for a piecewise-linear phase detector characteristic with $k = \frac{2}{\pi}$ in the parameter space for $K_{vco} > 0$, $\omega_e^{free} \geq 0$.

Based on the standard engineering analysis of the pull-in range with the help of numerical simulation, the boundary of global stability is determined as follows. For the fixed parameters $\tau_1 > 0$, $\tau_2 \geq 0$, $k > \frac{1}{\pi}$, and $K_{vco} > 0$, the trajectories from an arbitrary small neighborhood of an unstable equilibrium are monitored as $\omega_e^{free} \geq 0$ is sequentially increased in small steps until a bifurcation of the loss of global stability[5] is detected (see the vertical line in Fig. 3). Here, the disappearance of stable equilibria (for $0 < K_{vco} \leq K_{vco}^{ht}$; the green boundary segment on the left) and the birth of a saddle-to-saddle heteroclinic orbit (for $K_{vco}^{ht} < K_{vco} \leq K_{vco}^{pt}$; the blue boundary segment in the middle, when self-excited oscillations arise in the phase space) correspond to the trivial part of the boundary revealed in the standard analysis of the pull-in range. The birth of a semistable cycle (for $K_{vco} > K_{vco}^{pt}$; the red boundary segment on the right), which is a hidden oscillation, determines a hidden part of the global stability boundary that is not revealed by the standard analysis of the pull-in range (see Fig. 4) and is a counterexample to Kapranov's conjecture. The blue dashed curve depicts the "boundary" determined by the standard engineer-

[5] It is well known that system (1) with $\omega_e^{free} = 0$ is globally stable, which follows from the analysis of the Lyapunov function $V(u) = \frac{K_{vco}}{2\tau_1} u_1^2 + \int_0^{u_2} v_e(\sigma) d\sigma$.

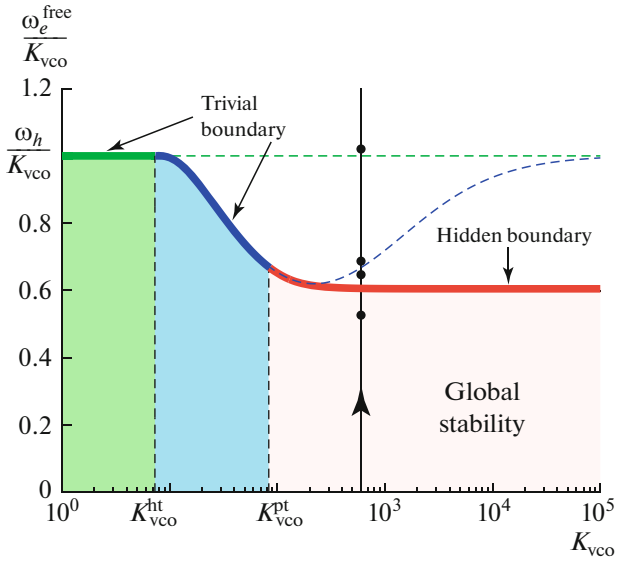

Fig. 3. Boundary of global stability constructed according to Theorem 2. The part of the boundary for sufficiently large K_{vco} corresponds to the asymptotic value $\frac{\omega_e^{\text{free}}}{K_{\text{vco}}} = 0.605$, according to Corollary 1. Parameters: $k = \frac{2}{\pi}$, $\tau_1 = 0.0448$, and $\tau_2 = 0.0185$.

ing analysis and Kapranov's conjecture, and the gap between the red boundary segment and the blue dashed curve shows the necessity of analyzing hidden oscillations in examining the global behavior of the system.

The circles in the vertical line $K_{\text{vco}} = 600$ in Fig. 3 denote the parameter values used to construct the phase portraits presented in Fig. 4. Here, the red upper trajectory $u_s(t)$ was constructed by the numerical integration from a neighborhood of an unstable equilibrium (without loss of generality, we used the trajectory of an unstable one-dimensional manifold, for which initial data are determined analytically). The black lower trajectory $u_h(t)$ was constructed analytically based on the features of the behavior of the system in Theorem 2.

Figure 4a ($\omega_e^{\text{free}} = 328.72 < \omega_p$) corresponds to the first point on the line of increasing $\omega_e^{\text{free}} \geq 0$ at which the red upper trajectory $u_s(t)$ from a neighborhood of an unstable equilibrium tends to an asymptotically stable equilibrium; initial data for the black lower trajectory $u_h(t)$ are chosen at the boundary of the absorbing set (6). In Fig. 4b ($\omega_e^{\text{free}} = 399.56 > \omega_p = \omega^{\text{pt}}$) the red upper trajectory $u_s(t)$ also tends to an asymptotically stable equilibrium (bifurcation of the birth of a saddle-to-saddle heteroclinic orbit has not yet happened: $\omega_e^{\text{free}} = 399.56 < \omega^{\text{ht}}$) without revealing the loss of global stability, because the system has a stable cycle of the second kind, which is a hidden oscillation arising due to the global bifurcation of the birth of a semistable cycle at $\omega_e^{\text{free}} = \omega^{\text{pt}}$. Note that direct numerical integration methods may also fail to detect a semistable cycle and close ones because of the finiteness of the step size [21]. The importance of visualizing hidden oscillations for supplementing Viterbi's simulation results [13] was noted in [9].

As ω_e^{free} increases further, $\omega_e^{\text{free}} = 399.77 > \omega^{\text{ht}} > \omega^{\text{pt}} = \omega_p$, the red upper trajectory $u_s(t)$ from the neighborhood of the unstable equilibrium tends to a stable cycle of the second kind (black lower trajectory $u_h(t)$) in Fig. 4c and shows the loss of global stability after the intersection of its boundary. For $\omega_e^{\text{free}} = 601 > K_{\text{vco}} = \omega_h$, the equilibrium states disappear and all the trajectories tend to a cycle of the second kind (Fig. 4d), showing the loss of global stability when tracked from a neighborhood of a stable equilibrium as well (external estimate of the global stability boundary).

5. CONCLUSIONS

In the general case, the simple structure of the global stability boundary obtained in the considered example corresponds to a manifold of one dimension lower (hypersurface) in the space of real parameters. For each point of this boundary, there is a neighborhood in the parameter space that is divided by the boundary into two connected open subsets, one containing only points of global stability, and the other, only points of no global stability. The type of a boundary point, hidden or trivial, is uniquely determined in this neighborhood along any continuous path of the intersection of the boundary through the point into the instability domain. The interiors of the largest connected subsets of boundary points of the same type define a partition of the global stability boundary into hidden and trivial domains (parts).

Trivial parts of boundaries can be revealed by applying well-developed methods for analysis of local bifurcations and numerical analysis of self-excited oscillations in a neighborhood of unstable points of the stationary set. Methods for revealing hidden parts of the global stability boundary require nonlocal analysis, including analysis of global bifurcations, and such methods are developed in the theory of hidden oscillations [4, 5]. Classical problems and conjectures on global stability by the first approximation (the Andronov–Vyshnegradsky problem [22], Aizerman's conjecture [23], Kalman's conjecture [24], Kapranov's conjecture, and others [4]) are associated with justifying and developing ideas concerning trivial boundaries of global stability.

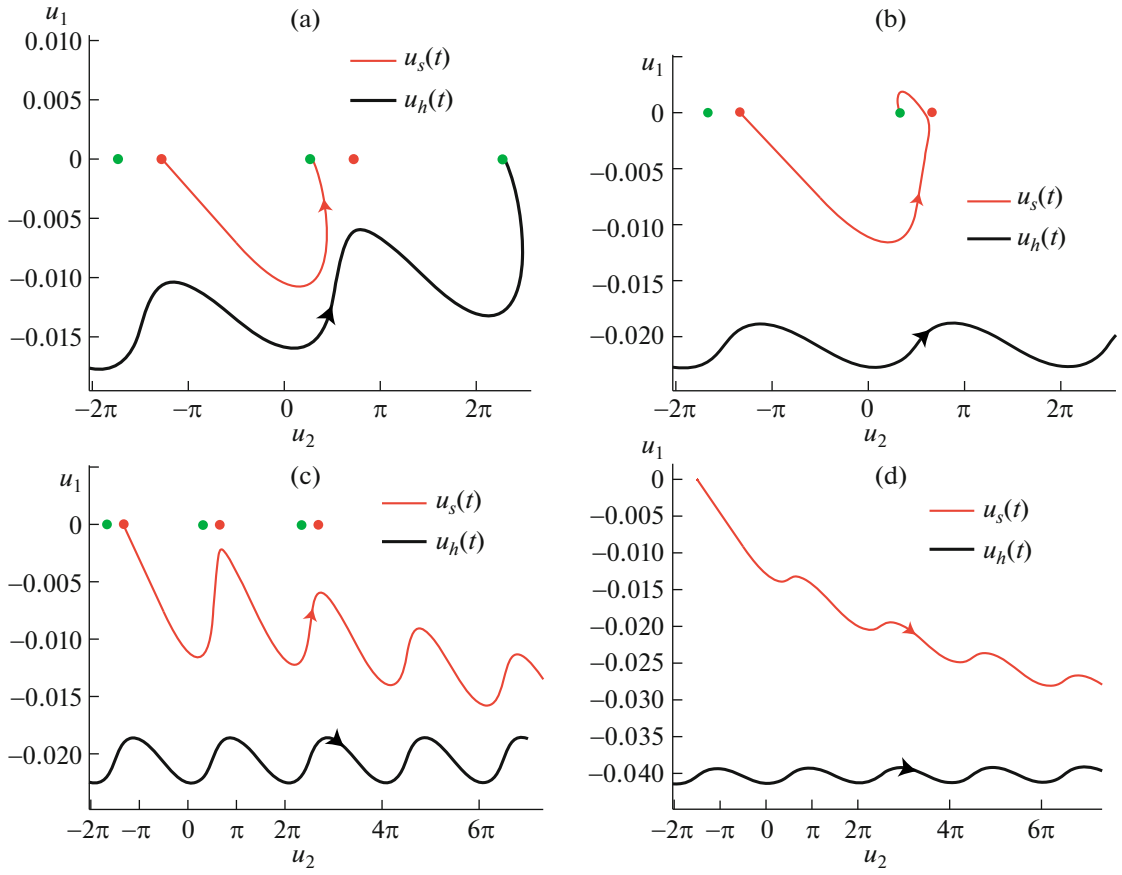

Fig. 4. Phase portraits of system (1) for parameter values $\tau_1 = 0.0448$, $\tau_2 = 0.0185$, $K_{\text{vco}} = 600$ and (a) $\omega_e^{\text{free}} = 328.72$, (b) $\omega_e^{\text{free}} = 399.56$, (c) $\omega_e^{\text{free}} = 399.77$, and (d) $\omega_e^{\text{free}} = 601$.

For PLL systems with higher order filters, internal (conservative) estimates for the global stability boundary can be obtained by generalizing Lyapunov's direct method and frequency-domain techniques to the cylindrical phase space (see [2, 5, 17, 25]).

FUNDING

This work was supported by the Russian Science Foundation, project no. 22-11-00172.

CONFLICT OF INTEREST

The authors declare that they have no conflicts of interest.

REFERENCES

1. V. V. Shakhgil'dyan and A. A. Lyakhovkin, *Phase-Locked Loops* (Svyaz', Moscow, 1972) [in Russian].
2. G. A. Leonov and N. V. Kuznetsov, *Nonlinear Mathematical Models of Phase-Locked Loops: Stability and Oscillations* (Cambridge Scientific, Cambridge, 2014).
3. G. A. Leonov, "Phase synchronization: Theory and applications," Autom. Remote Control **67**, 1573–1609 (2006).
4. N. V. Kuznetsov, "Theory of hidden oscillations and stability of control systems," J. Comput. Syst. Sci. Int. **59** (5), 647–668 (2020).
5. N. Kuznetsov, M. Lobachev, M. Yuldashev, R. Yuldashev, E. Kudryashova, O. Kuznetsova, E. Rosenwasser, and S. Abramovich, "The birth of the global stability theory and the theory of hidden oscillations," *2020 European Control Conference Proceedings* (2020), pp. 769–774.
6. M. V. Kapranov, "Pull-in range in phase-locked loops," Radiotekhnika **11** (12), 37–52 (1956).
7. F. Tricomi, "Integrazione di un'equazione differenziale presentatasi in elettrotecnica," Ann. Sc. Normale Super. Pisa **2** (2), 1–20 (1933).
8. N. A. Gubar', "Investigation of a piecewise linear dynamical system with three parameters," J. Appl. Math. Mech. **25** (6), 1519–1535 (1961).
9. C. Cahn, "Piecewise linear analysis of phase-lock loops," IRE Trans. Space Electron. Telemetry, No. 1, 8–13 (1962).

10. B. I. Shakhtarin, "Study of a piecewise-linear system of phase-locked frequency control," Radiotekh. Elektron., No. 8, 1415–1424 (1969).
11. V. M. Safonov, "Influence of a sawtooth phase detector characteristic on the pull-in range of a phase-locked loop," Radiotekhnika **24** (6), 76–80 (1969).
12. L. N. Belyustina, V. V. Bykov, K. G. Kiveleva, and V. D. Shalfeev, "On the magnitude of the locking band of a phase-shift automatic frequency control system with a proportionally integrating filter," Radiophys. Quantum Electron. **13**, 437–440 (1970).
13. A. Viterbi, *Principles of Coherent Communications* (McGraw-Hill, New York, 1966).
14. N. Margaris, *Theory of the Non-linear Analog Phase Locked Loop* (Springer, New Jersey, 2004).
15. M. V. Blagov, N. V. Kuznetsov, M. Yu. Lobachev, B. I. Shakhtarin, M. V. Yuldashev, and R. V. Yuldashev, "Nonlinear analysis and synthesis of a phase-locked loop: Kapranov's conjecture and hidden oscillations," *Proceedings of the 15th Multiconference on Control Problems* (2022), pp. 212–213.
16. N. Kuznetsov, D. Arseniev, M. Blagov, M. Lobachev, Z. Wei, M. Yuldashev, and R. Yuldashev, "The Gardner problem and cycle slipping bifurcation for type-2 phase-locked loops," Int. J. Bifurcation Chaos **32** (9), 2250138 (2022).
17. N. Kuznetsov, M. Lobachev, M. Yuldashev, and R. Yuldashev, "The Egan problem on the pull-in range of type 2 PLLs," IEEE Trans. Circuits Syst. II: Express Briefs **68** (4), 1467–1471 (2021).
18. G. Leonov, V. Reitmann, and V. Smirnova, *Nonlocal Methods for Pendulum-Like Feedback Systems* (Teubner, Stuttgart, 1992).
19. N. Kuznetsov, M. Lobachev, M. Yuldashev, R. Yuldashev, and M. Tavazoei, "The Gardner problem on the lock-in range of second-order type 2 phase-locked loops," IEEE Trans. Autom. Control (2023). https://doi.org/10.1109/TAC.2023.3277896
20. F. M. Gardner, *Phaselock Techniques*, 3rd ed. (Wiley, New York, 2005).
21. N. Kuznetsov, G. Leonov, M. Yuldashev, and R. Yuldashev, "Hidden attractors in dynamical models of phase-locked loop circuits: Limitations of simulation in MATLAB and SPICE," Commun. Nonlinear Sci. Numer. Simul. **51**, 39–49 (2017).
22. A. A. Andronov and A. G. Maier, "Vyshnegradskii problem in the theory of direct-acting regulators," Dokl. Akad. Nauk SSSR **47** (5), 345–348 (1945).
23. M. A. Aizerman, "On a problem concerning the global stability of dynamical systems," Usp. Mat. Nauk **4** (4), 187–188 (1949).
24. R. Kalman, "Physical and mathematical mechanisms of instability in nonlinear automatic control systems," Trans. ASME **79** (3), 553–566 (1957).
25. N. V. Kuznetsov, M. Yu. Lobachev, M. V. Yuldashev, and R. V. Yuldashev, "On the Gardner problem for phase-locked loops," Dokl. Math. **100** (3), 568–570 (2019).

Translated by I. Ruzanova